ISSN 0021-3640, JETP Letters, 2014, Vol. 100, No. 2, pp. 95–101. © Pleiades Publishing, Inc., 2014.
Original Russian Text © S.S. Aplesnin, M.N. Sitnikov, 2014, published in Pis'ma v Zhurnal Eksperimental'noi i Teoreticheskoi Fiziki, 2014, Vol. 100, No. 2, pp. 104–110.

Magnetotransport Effects in Paramagnetic $Gd_xMn_{1-x}S$

S. S. Aplesnin* and M. N. Sitnikov

Kirensky Institute of Physics, Siberian Branch, Russian Academy of Sciences, Akademgorodok, Krasnoyarsk, 660036 Russia
Siberian State Aerospace University, Krasnoyarsk, 660014 Russia
** e-mail: api@iph.krasn.ru*

Received June 2, 2014; in final form, June 11, 2014

The electrical resistance of $Gd_xMn_{1-x}S$ solid solutions with $x = 0.1$, 0.15, and 0.2 has been measured at magnetic field $H = 0.8$ T and at zero magnetic field within the 100 K $< T <$ 550 K temperature range. The magnetoresistance peak is observed above room temperature. On heating, the composition with $x = 0.2$ exhibits the change of magnetoresistance sign from positive to negative and the magnetoresistance peak near the transition to the magnetically ordered state. The experimental data are interpreted in the framework of the model involving the orbital ordering of electrons and the arising electrical polarization leading to the changes in the spectral density of states for electrons in the vicinity of the chemical potential in the applied magnetic field.

DOI: 10.1134/S0021364014140021

1. INTRODUCTION

The spin-dependent electron transport [1] is a basis of spintronic devices. An applied magnetic field affects the magnetic state of a multilayer nanostructure and controls the spin-polarized current due to the magnetoresistive effect. Manganites attract special attention of researchers [2] related to the possible formation of different types of inhomogeneous charge and spin states such as lattice and magnetic polarons and droplet and stripe structures. Similar phenomena are characteristic of many strongly correlated electron systems. The phase separation induced by doping can give rise to anomalies in the transport characteristics [3] resulting from changes in the local electron environment in the vicinity of such inhomogeneities affecting the charge carriers. Note that it is favorable for such inhomogeneities to be located as far as possible from each other to minimize the Coulomb energy [4].

The magnetoresistance in the paramagnetic state can result from the existence of degenerate orbital electron states and of strong electron correlations [5]. In particular, near the complete filling of the electron states, the orbital degeneracy is able to induce the long-range orbital order. For the latter, the probability to find an electron at one of the orbitals depends on both the lattice and orbital types. The orbital order can be accompanied by the lattice distortion, namely, by the Jahn–Teller distortions related to the electron–lattice coupling. At the same time, the orbitally ordered state can also be favorable in energy without any lattice distortions [5].

A high doping level can lead to the orbitally disordered state, which is favorable in energy in comparison to the antiferro-orbital state owing to the decrease in the kinetic energy. Similarly to the disordered spin systems, in which ferromagnetic polarons [3] exist in the paramagnetic state, here the orbital polarons contribute to the transport properties of the systems under study [6]. The shape of orbital polarons depends on the configurations of electron orbitals. They can have a disklike or chainlike shape depending on the ratio of the values of the exchange interaction between pseudo-orbital angular momenta and of the hopping integrals [6]. In the applied magnetic field, taking into account the electron phase, the energy of the disk-shaped orbital polaron is lower than that in the case of the chain. In the case of nonzero orbital magnetic moment, e.g., for electrons in t_{2g} states, the orbital polarons have a magnetic moment. In such a situation, the energy of an orbital polaron depends on the direction and magnitude of the applied magnetic field. As a result, a magnetoresistive effect is possible in the absence of static lattice distortions.

In manganese sulfide (MnS), the orbital degeneracy can arise at electron doping as a result of the replacement of a divalent manganese ion by trivalent rare-earth 4*f* elements, such as gadolinium ions existing in the metallic compound GdS [7] with the crystal and magnetic structures similar to those of MnS. Owing to strong electron correlations, MnS exhibits a 2.5-eV band gap. At certain values of the parameters, the interactions between 5*d* and 4*f* electrons lead to a decrease in the electron kinetic energy and favor the formation of the orbital ordering at gadolinium ions in the t_{2g} subsystem. The intra- and interatomic spin–orbit interaction, which can be enhanced by the electron–phonon interaction, leads to the spin-induced splitting in the spectrum of electron excitations.

The aim of this work is to reveal the mechanism of the magnetoelectric coupling for the orbitally degenerate electron states and to determine the correlation

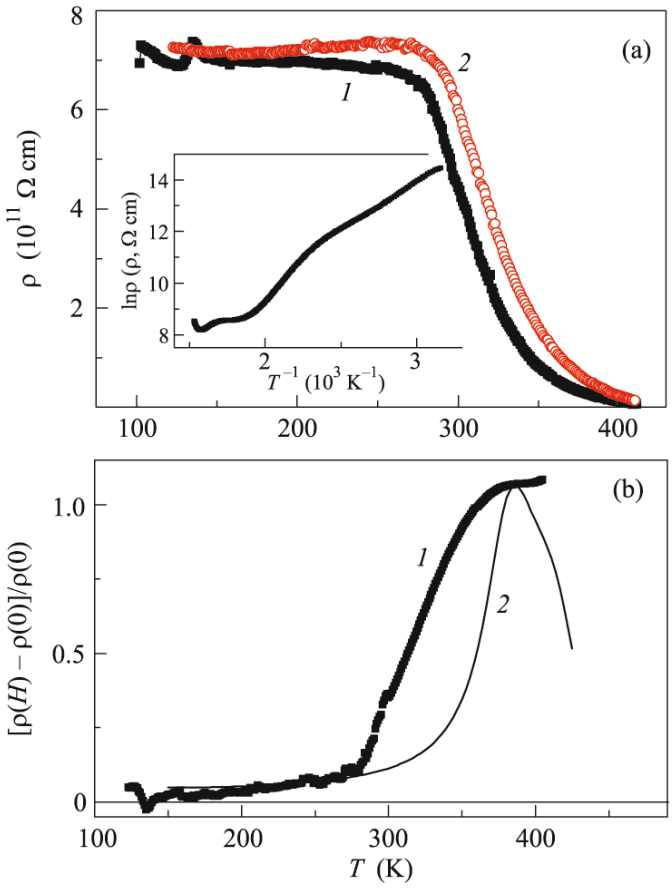

Fig. 1. (Color online) (a) Electrical resistivity of $Gd_{0.1}Mn_{0.9}S$ samples (*1*) at zero magnetic field and (*2*) in the applied magnetic field $H = 0.8$ T. (b) Temperature dependence of the resistivity in the applied magnetic field $[\rho(H) - \rho(0)]/\rho(0)$: (*1*) experimental data and (*2*) functions (1) and (3) calculated using the parameters $m_L^2 = 0.15$, $H_A/T_c = 0.4$, $\lambda = 0.005$, $T_{c,B} = 400$ K, $T_c = 500$ K, and $\Delta E = 0.3$ eV. The inset shows the plot of the logarithm of the resistivity versus inverse temperature at zero magnetic field.

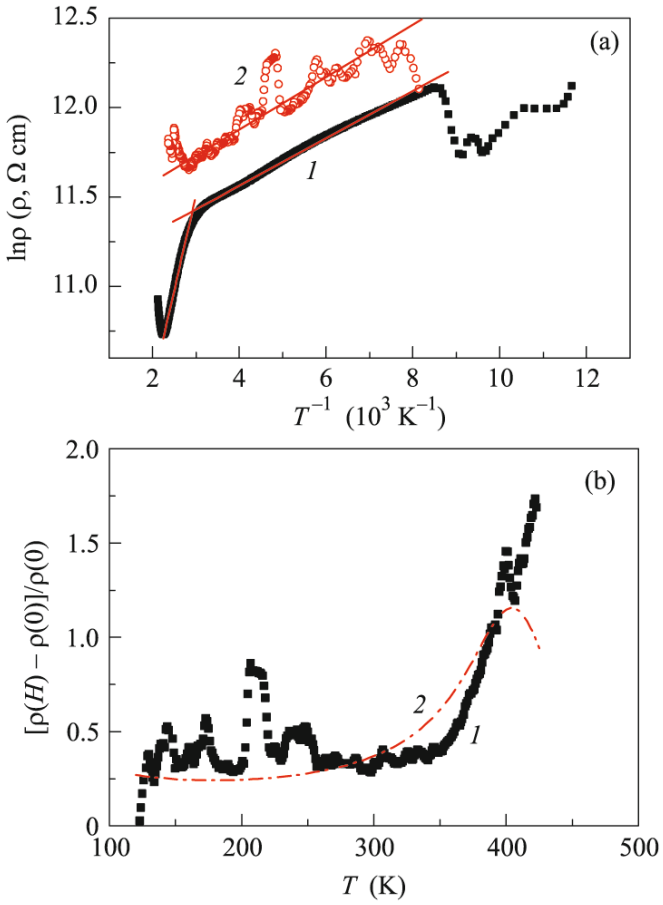

Fig. 2. (Color online) (a) Logarithm of the electrical resistivity of $Gd_{0.15}Mn_{0.85}S$ samples versus inverse temperature (*1*) at zero magnetic field and (*2*) in the applied magnetic field $H = 0.8$ T. (b) Temperature dependence of the resistivity in the applied magnetic field $[\rho(H) - \rho(0)]/\rho(0)$: (*1*) experimental data and (*2*) functions (1) and (3) calculated using the parameters $m_L^2 = 0.6$, $H_A/T_c = 0.1$, $\lambda = 0.02$, $T_{c,B} = 450$ K, $T_c = 460$ K, and $\Delta E = 0.12$ eV.

between the temperature and magnetic field dependences of the magnetic and transport characteristics in the applied magnetic field.

2. EXPERIMENTAL RESULTS

The synthesis of the $Gd_xMn_{1-x}S$ solid solutions and their X-ray diffraction analysis are described in detail in [8]. The magnetic and calorimetric measurements [9] revealed a decrease in the magnetic phase transition temperature from $T = 150$ K to $T(x = 0.2) = 120$ K and allowed determining the critical doping level corresponding to the decay of the long-range order and to the formation of a spin glass ($x_c = 0.23$). The measurements of electrical resistance were performed by the four-probe method in the applied magnetic field $H = 0.8$ T perpendicular to the electric current. The measurements were performed within the 100 K < T < 550 K temperature range using samples with the compositions $x = 0.1$, 0.15, and 0.2. In the case of $x = 0.1$ (Fig. 1), the electrical resistance varies with the temperature only slightly up to 260 K, and then it exponentially decreases, whereas the activation energy ΔE changes from 0.31 eV to 0.61 eV; the latter value corresponds to $T = 440$ K. On further heating (at $T > 550$ K), the electrical resistance is nearly independent of temperature. In the applied magnetic field, the electrical resistance increases. An especially steep increase is observed at $T > 270$ K. The magnetoresistance defined as $\delta = [\rho(H) - \rho(0)]/\rho(0)$ has a peak at $T = 400$ K (Fig. 1b).

In the case of $x = 0.15$ (Fig. 2), at the transition from the magnetically ordered phase to the paramagnetic state, the electrical resistance increases by 50%.

On further heating, we observe the change in the activation energy ΔE from 0.012 eV to 0.09 eV. The applied magnetic field induces the growth of the electrical resistance in the paramagnetic state by 40% accompanied by the growth of the magnetoresistance at temperatures above 360 K.

If the concentration of gadolinium ions within the 100 K < T < 550 K temperature range exceeds the percolation threshold $X_c = 0.16$, the electrical resistance of $Gd_xMn_{1-x}S$ solid solutions varies within one order of magnitude and has a minimum value at $T = 325$ K (Fig. 3). In the applied magnetic field, the electrical resistance also grows and the minimum in its temperature dependence is shifted toward higher temperatures up to $T = 380$ K. With the growth of the temperature (at $T = 320$ K), the magnetoresistance illustrated in Fig. 3b changes its sign from positive to negative. At 475 K, the magnetoresistance vanishes. An anomaly in the temperature dependence of the magnetoresistance is observed at $T \simeq 210$ K in the samples with two compositions near the doping level corresponding to the percolation threshold. This anomaly correlates with the anomaly in the temperature dependence of the relative change in the sample volume, which is observed within the T = 200–225 K temperature range (see inset in Fig. 3). This dependence has been obtained by the subtraction of the asymptotic continuation of the linear high-temperature function $\Delta V/V$ [9] at $T >$ 250 K from the total temperature dependence of the relative change in the sample volume. Below 250 K, the lattice starts to shrink and the electrical resistance increases. Probably, this is related to structural distortions of the crystal lattice. The magnetoresistance peak is observed in the vicinity of the transition to the magnetically ordered state and asymptotically disappears with the decrease in temperature. A possible cause of this peak stems from the phase separation and the formation of ferrons within the antiferromagnetic host material. Such a mechanism can be used to interpret the growth of the magnetic susceptibility on cooling. The magnetoresistance also manifests itself in the form of current–voltage curves measured at room temperature both at zero magnetic field and in the applied magnetic field $H = 0.8$ T (Fig. 4). With the increase in the electrical current, the magnetoresistance exhibits a peak and then steeply decreases at an electrical current of 1 mA and a voltage of 1 V.

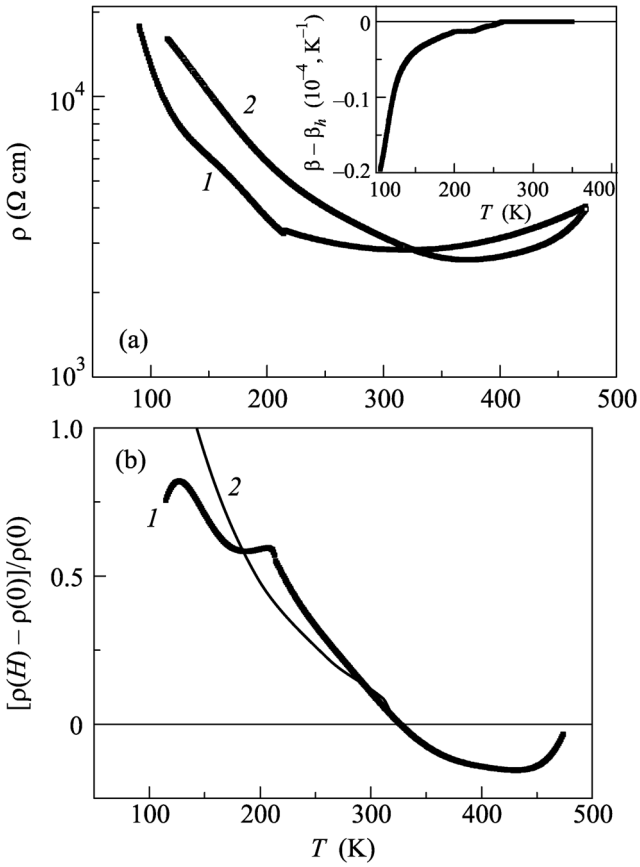

Fig. 3. (a) Electrical resistivity of $Gd_{0.2}Mn_{0.8}S$ samples (*1*) at zero magnetic field and (*2*) in the applied magnetic field $H = 0.8$ T. (b) Temperature dependence of the resistivity in the applied magnetic field $[\rho(H) - \rho(0)]/\rho(0)$: (*1*) experimental data and (*2*) function (4) calculated using the parameters T_c = 500 K, $T_{c,Mn}$ = 420 K, and $T_{c,Gd}$ = 320 K. Inset shows the relative change in the sample volume determined by the subtraction of the extrapolated linear function $\Delta V/V(T)$ at $T > 250$ K from the temperature dependence of $\Delta V/V(T)$.

3. MODEL

To interpret the experimental data, we assume that an electron tunnels from a gadolinium ion to the 3*d* band formed by the nearest manganese ions and orbital ordering arises at manganese and gadolinium ions. The spin–orbit interaction in the manganese subsystem is related to the electron doping and lifting the degeneracy in the t_{2g} subband owing to the interatomic interactions. The change in the symmetry of the electron density at a cation leads to a modification of phonon vibration modes in the octahedron. The splitting of these modes near the Brillouin zone boundary leads to a change in the permittivity and to the electrical polarization of the regions in the vicinity of the interface between Mn and Gd ions.

The electrical resistance below room temperature results from the tunneling of electrons and is independent of temperature. With the growth of the temperature, the impurity conductivity related to gadolinium ions, which play the role of donors for Mn^{2+} ions, begins to prevail. At $x = 0.1$, the orbital polarons become pinned at $T = 400$ K and the magnetic moments of electrons form superparamagnetic particles. Similar to the spin systems, where the fluctuations of spin density described in terms of a short-range magnetic order lead to the displacement of the mobility edge and the growth of the electrical resistance, here we use the short-range order in the orbital

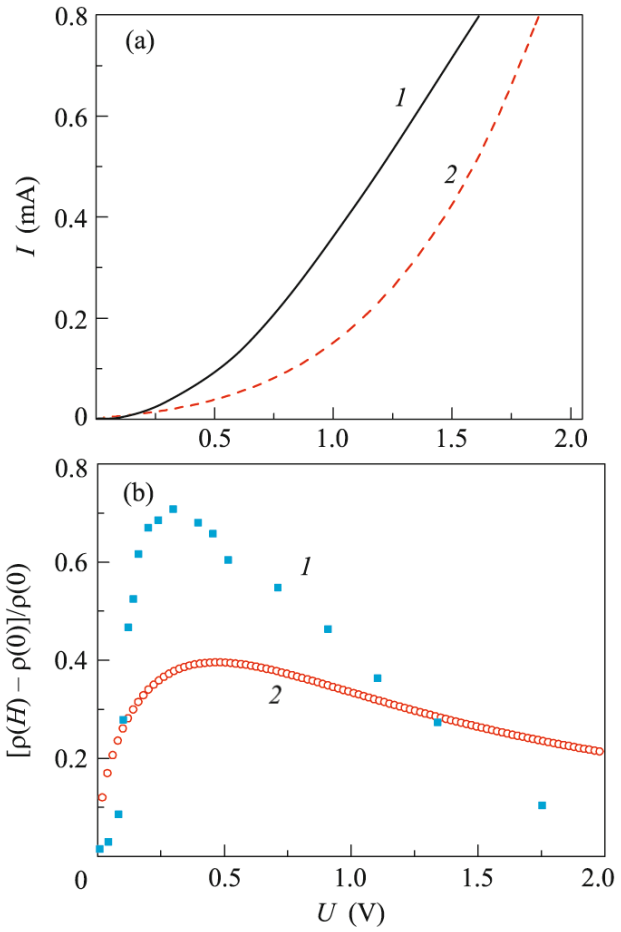

Fig. 4. (Color online) (a) Electrical current versus the applied voltage in the applied magnetic field $H = (1)$ 0 and (2) 0.8 T. (b) (1) Measured electrical resistance in the applied magnetic field $H = 0.8$ T versus the applied voltage at room temperature for the samples with $x = 0.2$ and (2) calculations according to Eq. (5) using the parameters $m_L = 0.06$ A/m, $P_0 = 0.02$ C/m^2, and $A = 100$ m^3/(C A).

subsystem, which is described by the correlation functions of orbital magnetic moments [9] and modifies the width of the conduction band, $[1 - \langle L(0)L(r)\rangle]W$. The electron ordering at certain orbitals leads to the anisotropy of hopping integrals and the narrowing of the conduction band, i.e., to an increase in the energy needed for the activation of charge carriers from the impurity level to the bottom of the conduction band. At low temperatures, the orbital magnetic moments of clusters are oriented chaotically and the correlation function $\langle L(0)L(r)\rangle$ tends to zero. On heating, the orbital magnetic moments try to orient themselves along the direction of the applied magnetic field; this leads to the growth of $\langle L(0)L(r)\rangle$. The change in the electrical resistance ρ in the applied magnetic field can be written as

$$[\rho(H) - \rho(0)]/\rho(0) = \exp[\langle L_H(0)L_H(r)\rangle - \langle L_0(0)L_0(r)\rangle]\Delta E/k_B T - 1, \quad (1)$$

where $\langle L_H(0)L_H(r)\rangle$ and $\langle L(0)L(r)\rangle$ are the orbital correlation functions in the presence and absence of the applied magnetic field, respectively. Further on, we estimate these correlation functions using the model of a superparamagnetic material in the presence of the applied magnetic field H and the anisotropy field H_A. We represent the energy of superparamagnetic particles as $W = M_L H\cos\theta + M_L H_A\cos(\gamma - \theta)$, where the angle θ specifies the direction of the orbital magnetic moment with respect to the applied magnetic field and γ is the angle between the directions of the applied magnetic field and the anisotropy field. The equilibrium direction of the orbital magnetic moment is determined by the expression $\tan\theta = H_A\sin\gamma/(H + H_A\cos\gamma)$. The change in the orbital magnetic moment of all particles in the applied magnetic field can be represented as

$$M_L^0\Delta\theta = M_L^0(\langle\cos\theta\rangle_H - \langle\cos\theta\rangle_0) = M_L^0 \times \left(\sum_i \frac{1}{\sqrt{1 + \dfrac{H_A^2\sin^2\gamma_i}{(H + H_A\cos\gamma_i)^2}}} - \frac{1}{\sqrt{1 + \tan^2\gamma_i}}\right). \quad (2)$$

At the random scatter of anisotropy axes within the $0 < \gamma < \pi$ angular range, the correlation function of orbital magnetic moments is small. We express the temperature dependence of this correlation function in terms of the orbital magnetization of a cluster and the angle between the directions of the moments

$$\langle L_H(0)L_H(r)\rangle - \langle L_0(0)L_0(r)\rangle = (M_L^0)^2\Delta(\theta) = m_L^2(1 - T/T_c)^{0.6} \times \left(\sum_i \frac{1}{\sqrt{(1 + \sin^2\gamma_i)/\left[\dfrac{\lambda}{(1 - T/T_{c,B})^2} + \cos\gamma_i\right]^2}} - \frac{1}{\sqrt{1 + \tan^2\gamma_i}}\right), \quad (3)$$

where $\lambda = H/K$ and K is the anisotropy constant. In three-dimensional anisotropic systems, the magnetization in the transition region has the form $M = m_L(1 - T/T_c)^\beta$, where $\beta = 0.3$–0.33. The anisotropy field also has a power-law temperature dependence, $H_A = K(1 - T/T_{c,B})^n$. The experimental curves are fitted better by the curve corresponding to the exponent $n = 2$. For $x = 0.1$, the experimental data on the magnetoresistance (see Fig. 1) are rather well fitted by functions (1) and (3) with the following parameters:

the orbital magnetic moment squared of a cluster $m_L^2 = 0.15$, anisotropy field $H_A/T_c = 0.4$, $\lambda = 0.005$, the pinning temperature for orbital polarons with the formation of clusters $T_{c,B} = 400$ K, the temperature corresponding to the formation of orbital polarons characterized by the short-range orbital order $T_c = 500$ K, and the activation energy $\Delta E = 0.3$ eV. With the growth of the concentration of gadolinium ions, the correlation functions for orbital magnetic moments also increase. For the sample with $x = 0.15$, we have $m_L^2 = 0.6$, the anisotropy field decreases ($H_A/T_c = 0.1$), $\lambda = 0.02$, the pinning temperature for orbital polarons $T_{c,B} = 450$ K approaches the temperature of their formation $T_c = 460$ K, and the activation energy is $\Delta E = 0.12$ eV. The theoretical results obtained using this model agree rather well with the experimental data on the magnetoresistance (see Fig. 2).

At $x = 0.2$, gadolinium ions form a percolation cluster in the lattice. In this case, we can separate two subsystems, of manganese and gadolinium, which at the Mn–Gd interface have polarization charges, which are characterized by the polarization vectors $\mathbf{P}_1$ and $\mathbf{P}_2$ related to each other via the orbital degrees of freedom of electrons, $M_L[P_1, P_2]$. As a result, we have two degenerate spirals with clockwise and counterclockwise rotation with different signs of the direction of the orbital magnetic moment. The applied magnetic field lifts the degeneracy with respect to the direction of the polarization vector ($M_L[P_1, P_2]$ and $-M_L[P_1, P_2]$) and leads to the enhancement of the total electric field in the sample. Eventually, the bottom of the conduction band is shifted with respect to the chemical potential. Thus, the change in the electrical resistance in the applied magnetic field can be written as

$$\begin{aligned}[\rho(H) - \rho(0)]/\rho(0) &= \exp\left(\frac{M_L[P_1, P_2]}{M_{0L}P_0^2}\frac{\Delta E}{k_B T}\right) - 1 \\ &= \exp\left[(1 - T/T_c)^{0.3} PP \frac{\Delta E}{k_B T}\right] - 1, \\ PP &= (1 - T/T_{c,\mathrm{Mn}})^{0.3}(1 - T/T_{c,\mathrm{Gd}})^{0.3},\end{aligned} \tag{4}$$

where M_L is the orbital magnetization; P_0 is the polarization vector; $T_{c,\mathrm{Mn}}$ and $T_{c,\mathrm{Gd}}$ are the critical temperatures corresponding to the vanishing of the polarization in the manganese and gadolinium subsystems, respectively; and T_c is the critical temperature for the formation of the orbital order. The experimental data on the magnetoresistance shown in Fig. 3 are fitted well by Eq. (4) with the following parameters: $T_c = 500$ K, $T_{c,\mathrm{Mn}} = 420$ K, $T_{c,\mathrm{Gd}} = 320$ K, and $\Delta E = 13$ meV. In the framework of the model under study, we can also describe the dependence of the magnetoresistance on the electric field, which tends to rotate the polarization vectors along the field, whereas the effective coupling with the orbital magnetic moments impedes this process. At high fields, the directions of the polarization vectors coincide with each other, and the coupling between the magnetic and electrical subsystems disappears. This can be illustrated using a simple model with the energy written as $AM_L[P_1, P_2] + E(P_1 + P_2)$. For the orthogonal configuration of the fields ($\mathbf{H} \perp \mathbf{E}$), expression $AM_L(P_{1x}P_{2y} - P_{1y}P_{2x} + E(P_{1y} + P_{2y})$ has a minimum at $\sin\varphi = -\frac{E}{4M_L P_0 A} + \sqrt{\frac{E^2}{16M_L^2 P_0^2 A^2} + 1}$. The dependence of the magnetoresistance on the electric field is determined by the angle φ

$$\begin{aligned}&[\rho(H) - \rho(0)]/\rho(0) \\ &= \exp(\sin\varphi\sqrt{1 - \sin^2\varphi}\Delta E/(k_B T)) - 1; \\ &\sin\varphi = -\frac{E}{4M_L P_0 A} + \sqrt{\frac{E^2}{16M_L^2 P_0^2 A^2} + 1},\end{aligned} \tag{5}$$

where A is the parameter characterizing the coupling between the orbital magnetic moment and the polarization vector and $E = U/d$ is the electric field. The canting angle of the sublattices formed by polarization vectors decreases with the growth of the electric field. At an angle of $\pi/2$, the magnetoresistance has a peak. At further rotation of the vectors toward the direction of the electric field, the coupling between the orbital magnetic moment and the electric dipole becomes weaker. Therefore, the magnetoresistance also decreases. The theoretically determined field dependence of the magnetoresistance shown in Fig. 4 is in qualitative agreement with the experimental data. The existence of the orbital order is confirmed by the magnetic measurements. It follows from the temperature dependence of the magnetic susceptibility (Fig. 5a). Within the 550 K $< T <$ 650 K temperature range, the magnetic susceptibility obeys the Curie–Weiss law with the paramagnetic Curie temperature $\theta = -108$ K. Below 550 K, we observe deviations of $\chi(T)$ from the Curie–Weiss law (the function $\Delta\chi = \chi^{ex} - \chi^{CW}$ is plotted in Fig. 5b). The total susceptibility can be represented as a sum $\chi = \chi_s + \chi_o + \chi_{so}$, where χ_s is the magnetic susceptibility of localized spins and χ_o and χ_{so} are the orbital and mixed susceptibilities, respectively. Below the temperature of the transition to the orbitally ordered state, the spin and mixed susceptibilities do not obey the Curie–Weiss law and depend on the orbital ordering parameter M_L whose temperature dependence is described by the power-law function (4).

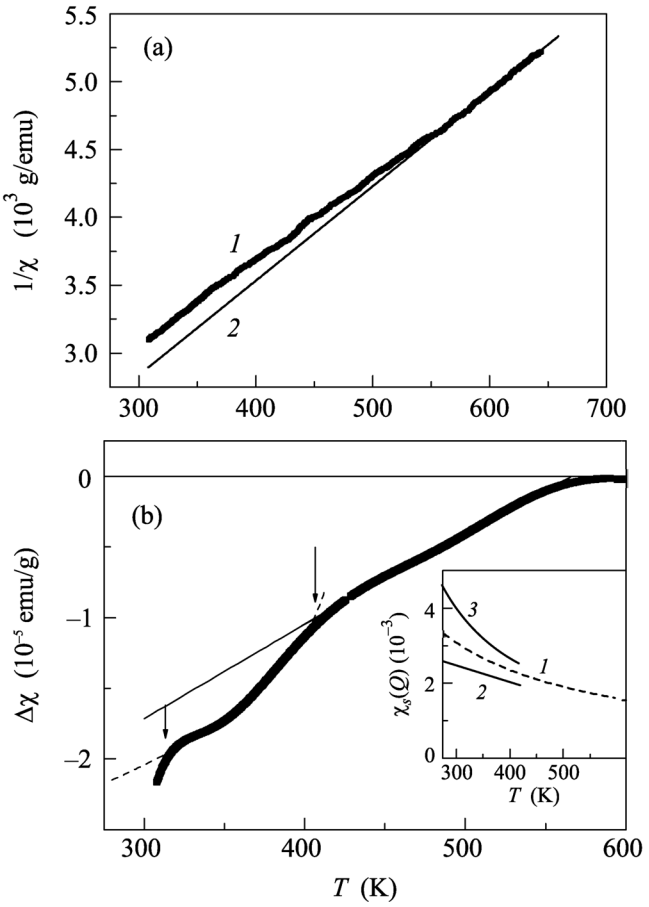

Fig. 5. Temperature dependences of (a) (*1*) the inverse magnetic susceptibility for $Gd_{0.2}Mn_{0.8}S$ sample and (*2*) the Curie–Weiss curve for the magnetic susceptibility and (b) their difference $\Delta\chi = \chi^{ex} - \chi^{CW}$. Inset shows the spin susceptibility at $T < T_c$ calculated by Eq. (6) using the parameters $J_s = -110$ K, $M_L = m_L(1 - T/T_c)^{0.3}$, and $J_m =$ (*2*) 100 and (*3*) –100 K and (*1*) the Curie–Weiss relation $\chi_s(Q) = 1/[T - J_s(Q)/4]$ [11].

The spin susceptibility at the wave vector characteristic of the structure under study has the form [11]

$$\chi_s(Q) = \frac{T + J_m(Q)/4(1 - 4M_L^2)}{T^2 + \frac{T}{4}[J_m(Q) - J_s(Q)] - 9/4J_mJ_s(1 - M_L^2)}, \quad (6)$$

where J_m is the Fourier transform of the exchange integral characterizing the exchange interaction between spin and orbital moments and $J_s(Q)$ is the exchange integral between spins at wave vector $Q = \pi$. The spin susceptibility χ_s is enhanced for the exchange parameter $J_m < 0$ and decreases at $J_m > 0$ below the temperature of the transition to the orbitally ordered state (see inset in Fig. 5b).

In [5], in the framework of the Hubbard model in the limit of strong electron correlations, the phase diagram describing the magnetic and orbital ordering was calculated and the semiconductor type of electrical conductivity was found, exhibiting a peak in the vicinity of the transition to the orbitally ordered state. On cooling, the electrical resistance in the applied magnetic field decreases and has a minimum near the orbital ordering temperature. The magnetoresistance attains the maximum value and then changes sign at the Curie temperature. The theoretical calculations of the magnetoresistance with the parameter of the on-site Coulomb interaction between electrons at the same orbital $U/W = 4$, the Hund's rule coupling constant $J/W = 1.2$, the interorbital Coulomb interaction $U' = U - 2J$, and the applied magnetic field $H/W = 0.001$ (where W is the band width) are in qualitative agreement with our experimental data for $x = 0.2$.

The orbital ordering in the $Gd_xMn_{1-x}S$ solid solution is confirmed by a broad peak in the specific heat at $T = 380$ K in the curve obtained by the subtraction of the phonon contribution from the measured temperature dependence of the specific heat [9]. The difference in the values of the critical temperature obtained from the data on the specific heat and magnetoresistance results from the fact that the specific heat peak is related to the decay of the long-range order, whereas the magnetoresistance is observed above the critical temperature and is determined by the short-range orbital order and vanishes at higher temperatures. In interpretation of the magnetoresistance data, we used the molecular field approximation, which gives higher values for critical temperatures in comparison to the model calculations taking into account the short-range order.

4. CONCLUSIONS

In this work, we have determined the magnetoresistance at temperatures exceeding by several times the temperature characterizing the transition to the magnetically ordered state in $Gd_xMn_{1-x}S$ solid solutions with $x = 0.1$, 0.15, and 0.2. For all compositions, we observe the semiconductor type of electrical conductivity with a small minimum in the high temperature range. The growth of the electrical resistance and of the activation energy in the applied magnetic field results from the growth in the field of the correlations between orbital magnetic moments. The coupling of orbitally ordered electrons with the vibration modes of the octahedra leads to the electrical polarization and to the dependence of the magnetoresistance on the applied electric field. Using the current–voltage curve, we find the magnetoresistance peak in both the electric current and voltage.

This work was supported by the Russian Foundation for Basic Research (project nos. 12-02-00125-a and 14-02-90010-Bel_a).

REFERENCES

1. A. Fert, Rev. Mod. Phys. **80**, 1517 (2008).
2. N. V. Volkov, Phys. Usp. **55**, 250 (2012).
3. M. Yu. Kagan and K. I. Kugel, Phys. Usp. **44**, 553 (2001); M. Yu. Kagan, A. V. Klaptsov, I. V. Brodskii, K. I. Kugel, A. O. Sboichakov, and A. L. Rakhmanov, Phys. Usp. **46**, 851 (2003).
4. A. L. Rakhmanov, K. I. Kugel, Ya. M. Blanter, and M. Yu. Kagan, Phys. Rev. B **63**, 174424 (2001).
5. R. Peters and N. Kawakami, Phys. Rev. B **83**, 125110 (2011).
6. K. I. Kugel, A. L. Rakhmanov, A. O. Sboychakov, and D. I. Khomskii, Phys. Rev. B **78**, 155113 (2008).
7. S. Kar, W. L. Boncher, D. Olszewski, N. Dollahon, R. Ash, and S. Stoll, Am. Chem. Soc. **132**, 13960 (2010).
8. O. B. Romanova, L. I. Ryabinkina, V. V. Sokolov, A. Yu. Pichugin, D. A. Velikanov, D. A. Balaev, A. I. Galyas, O. F. Demidenko, G. I. Makovetskii, and K. I. Yanushkevich, Solid State Commun. **150**, 602 (2010).
9. S. S. Aplesnin, O. B. Romanova, M. V. Gorev, D. A. Velikanov, A. G. Gamzatov, and A. M. Aliev, J. Phys.: Condens. Matter **25**, 025802 (2013).
10. P. Pfeffer and W. Zawadski, Phys. Rev. B **59**, R5312 (1999).
11. E. L. Nagaev, *Magnets with Complex Exchange Interactions* (Nauka, Moscow, 1988) [in Russian].

Translated by K. Kugel